FISEVIER

Contents lists available at ScienceDirect

Journal of Constructional Steel Research

journal homepage: www.elsevier.com/locate/jcsr



Simplified seismic design procedure for steel MRF structure with nonlinear viscous dampers



Baiping Dong a,*, James M. Ricles b

- a State Key Laboratory of Disaster Reduction in Civil Engineering & Department of Structural Engineering, Tongji Univ., Shanghai 200092, China
- b ATLSS Engineering Research Center, Dept. of Civil and Environmental Engineering, Lehigh Univ., Bethlehem, PA 18015, United States of America

ARTICLE INFO

Keywords:
Nonlinear viscous damper
Steel MRF
Simplified design procedure
Performance-based seismic design

ABSTRACT

This paper presents a simplified design procedure (SDP) for performance-based design of low-rise new steel MRF buildings with nonlinear viscous dampers. The SDP uses an effective stiffness and equivalent damping for a multi degree-of-freedom (MDOF) model of the MRF building, which is established using a linearized model of the damping system (damping devices and the associated bracing). The SDP is an integrated design process for the steel MRF and the damping system to achieve target performance objectives. The SDP is consistent with the analysis procedures in ASCE 7–16 for seismic design of conventional structures without dampers, however, differentiated from the analysis procedures for structures with dampers without the computation of effective period and effective damping ratio as a function of the ductility demand on the structure. The SDP was validated using nonlinear dynamic time history analyses (NDTHA) results for a 4-story example steel MRF building with nonlinear viscous dampers with two scenarios of damper arrangements in the building. The MRFs were designed for various base shear design strength levels (i.e., 100%, 75%, 60%, 50% and 40% of the required base shear design strength of ASCE 7–16), and nonlinear viscous dampers were sized and added to the MRFs to control the story drift response. The results presented in this paper show that performance objectives for the SDP can be selected and achieved using a MRF designed with smaller base shear design strength than a conventional MRF.

1. Introduction

Literature demonstrates that passive damping systems reduce inelastic deformation demands and damage in buildings under earthquake ground motions [1-5]. The earliest seismic design guidelines for buildings with damping systems directed the use of passive damping systems toward high-performance structures, that is, the seismic load resisting frames are designed to meet the strength and drift requirements of current seismic codes and the damping system is used to improve performance [4]. FEMA-273 presents guidelines for retrofitting existing buildings with damping systems [6]. For the design of new buildings with damping systems, the NEHRP provisions present linear analysis and design procedures for new buildings with damping systems [7,8]. Details and an assessment of these procedures are presented in literature [5,9-11]. These procedures adopt an equivalent linear system model where the maximum response of the highly damped nonlinear structure is estimated as the maximum response of an "equivalent" highly damped linear-elastic system with its stiffness equal to the secant stiffness taken to the maximum displacement of the nonlinear system [12,13].

As a code reference for new design and retrofit of building using damping system, ASCE 7-16 [14] gives the design requirements for a structure with added dampers. Basically, the ASCE 7-16 requirements for a structure with a damping system have two objectives: (1) achieving life safety, and (2) limiting damage to the seismic force-resisting system (SFRS) in a major earthquake. To meet the first performance objective, the damping system (damping devices and the associated bracing to transfer forces from the damping devices to the seismic mass degrees-offreedom (DOF)) is required to sustain forces associated with MCE ground motions. To meet the second performance objective, minimum design criteria, comparable to those for a structure with a conventional SFRS, are provided. ASCE 7-16 addresses these objectives with three principal design requirements: (a) Structures with a damping system are required to have a SFRS that provides a complete force path. The SFRS must comply with the design requirements of ASCE 7-16, except that the damping system may be used to meet drift limits. (b) The base shear design strength used to design the SFRS should not be less than 75% of the base shear design strength used to design a similar conventional SFRS without dampers. (c) Components of the damping system, other

E-mail addresses: baipingdong@tongji.edu.cn (B. Dong), jmr5@lehigh.edu (J.M. Ricles).

^{*} Corresponding author.

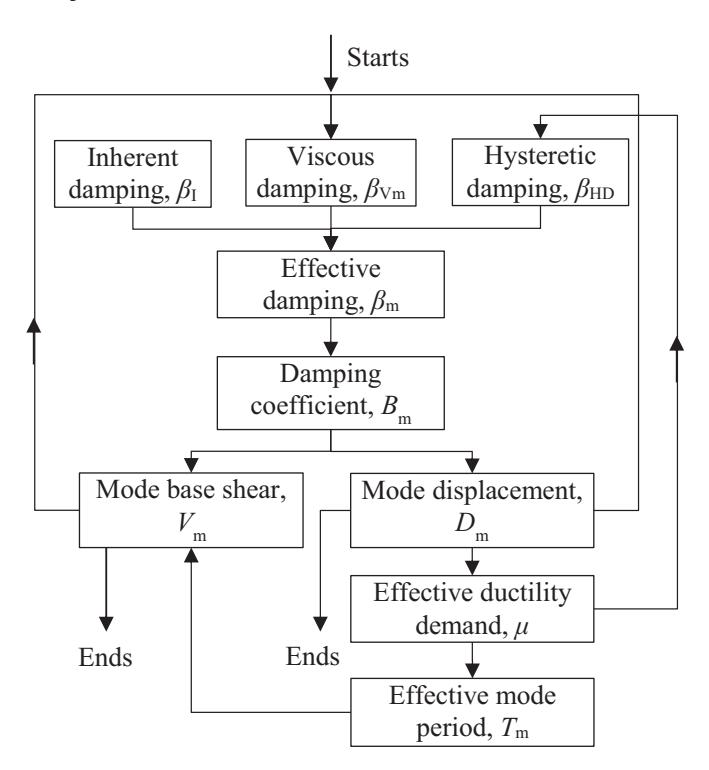


Fig. 1. ASCE 7-16 analysis procedure for structure with added dampers.

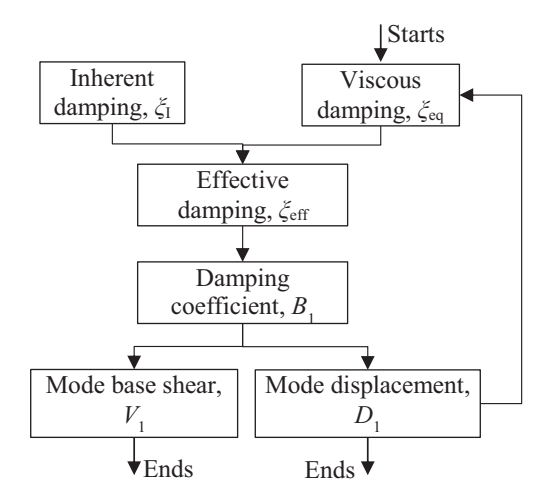


Fig. 2. Schematic of simplified design procedure (SDP) for MRF with nonlinear viscous dampers.

than damping devices, should be designed to remain essentially elastic for design forces including the forces from the damping devices.

ASCE 7–16 also outlines linear analysis procedures (i.e., the equivalent lateral force (ELF) procedure and the response spectrum analysis (RSA) procedure) and a nonlinear analysis procedure (i.e., the nonlinear time history response analysis procedure) for seismic design of a structure with added damping devices. These RSA and ELF procedures are compatible with nonlinear static analysis procedures of FEMA 440 [15] for conventional structures [11,16]. The ELF and RSA procedures are permitted for a structure with a damping system when: (1) the damping system has at least two damping devices in each story in the direction of interest, which are configured to resist torsion; (2) the total effective damping of the fundamental mode of the structure in the direction of interest is not greater than 35% percent of critical; and (3) the usual limitations for using the ELF and RSA procedures for conventional structures are satisfied. According to ASCE 7–16, the effective stiffness

(i.e., secant stiffness) and effective damping (i.e., including inherent damping, viscous damping, and hysteretic damping) at the effective fundamental period of the structure should be used in either the ELF or RSA procedure. The effective stiffness should be based on an idealized nonlinear characterization (i.e., idealized pushover capacity curve expressed in terms of base shear and roof displacement) of the structure. The assumption is that structures with damping devices are expected to yield during a strong earthquake ground motion, and therefore, the hysteretic damping from the post-yield hysteretic behavior of the SFRS, as well the damping effect of the damping devices, should be included. Fig. 1 shows a schematic of the procedure, which requires an iterative process to obtain the final base shear and displacement depending on the effective period, ductility demand, and effective damping.

The study investigates if the RSA and ELF procedures could be simplified, to eliminate the need for nonlinear analysis. To simplify the analysis process for seismic design of a steel MRF building with nonlinear viscous dampers, a simplified design procedure (SDP) is proposed, shown schematically in Fig. 2. The SDP is based on the equal displacement approximation [17], under the assumption that limited ductility demand on the SFRS is expected under DBE and MCE level ground motions, so that the equal displacement approximation is expected to be reasonably accurate. The equal displacement approximation suggests that the response coefficients include the response modification factor, R, and the displacement amplification factor, C_d, used to estimate the strength and displacement demands on a SFRS that is designed using linear analysis methods are equal to the ductility demand, μ , of the SFRS, i.e., $R = C_d = \mu$. The SDP is expected to be compatible with and provide accuracy similar to the linear-analysisbased procedures of ASCE 7-16 for conventional SFRS.

2. Simplified design procedure (SDP)

2.1. Overview of SDP

To be consistent with the analysis procedures in ASCE 7-16 for seismic design of conventional structures without dampers, the SDP uses an analysis of a linear model of the seismic force-resisting system (SFRS) (i.e., the MRF) and an equivalent linearized model of the damping system. Unlike the current analysis procedures for a structure with added dampers in ASCE 7-16, where the effective period and effective damping ratio are computed as a function of the ductility demand on the structure, the SDP has the following characteristics: (1) The SDP performs an integrated design of the steel MRF and the damping system (e. g., damping devices and the associated bracing) for performance objectives defined in terms of story drift. (2) The SDP uses the initial stiffness of a linear elastic model of the MRF to determine the mode shapes and natural frequencies (periods) of the system. (3) The SDP includes the flexibility of the damping system and idealizes the nonlinear viscous damper and associated bracing (termed the nonlinear viscous damper-brace component) as an equivalent linear elastic-viscous model. (4) The SDP uses an estimate of the effective period and effective equivalent damping of the MRF with the damping system based on the initial stiffness of the MRF, the inherent damping of the building, and the equivalent stiffness and equivalent viscous damping of the linear elastic-viscous model. (5) The SDP uses the equal displacement approximation to predict the displacement response (i.e., $C_d = R = \mu$) and does not include a complex calculation of the ductility demand and associated hysteretic damping of a nonlinear model of the MRF as in current procedures of ASCE 7-16. (6) The SDP uses the ELF or RSA procedure for linear analysis of the MRF with the damping system, which is consistent with the current analysis methods in ASCE 7–16 for a conventional MRF.

2.2. Steps of SDP

Fig. 3 shows the schematic of the SDP. The steps of the SDP are as follows:

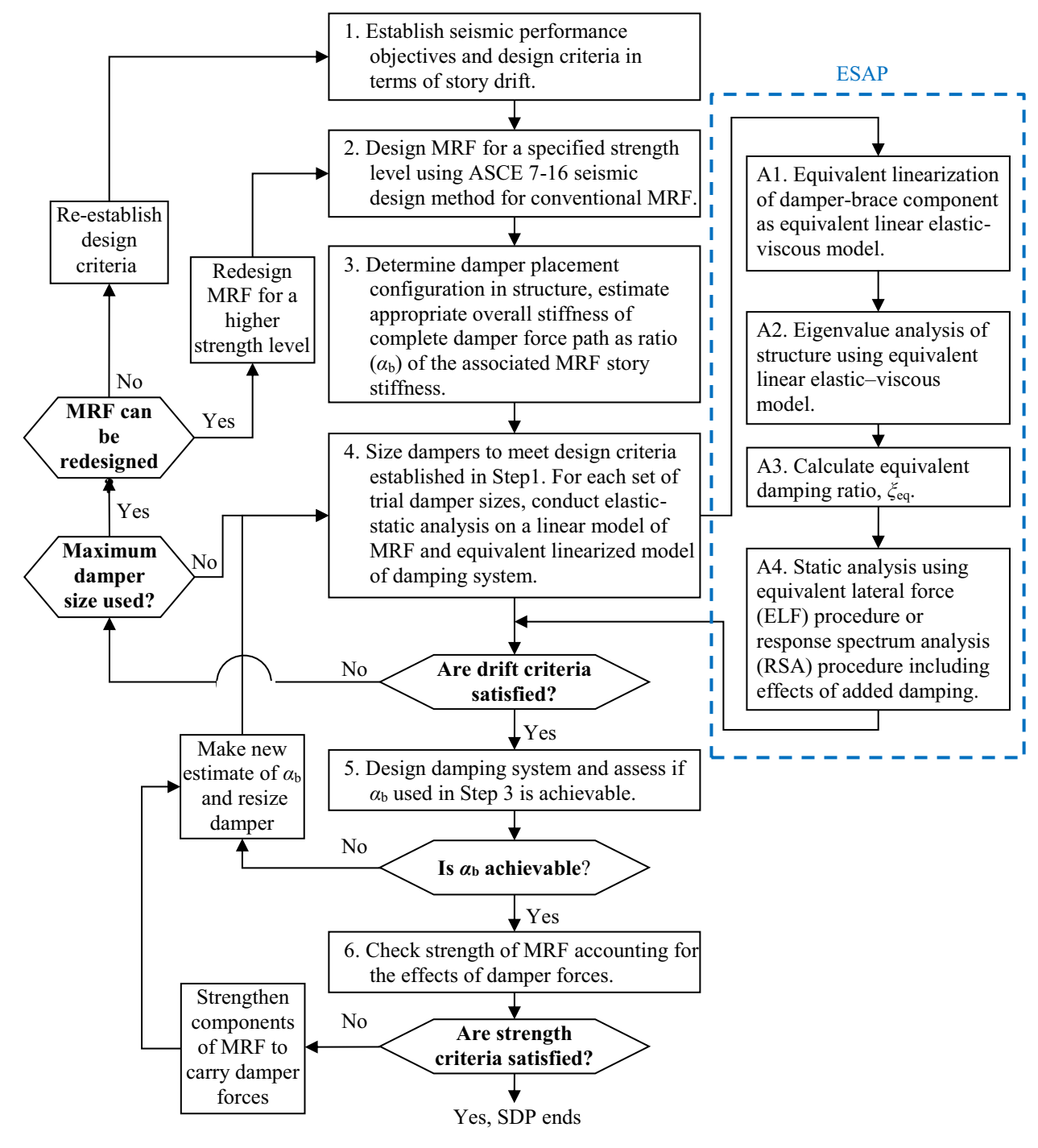


Fig. 3. Simplified design procedure (SDP) for MRF with nonlinear viscous dampers.

Step 1.Establish target seismic performance objectives and design criteria in terms of story drift. Performance objectives specified in ASCE 41–06 [18] can be considered, such as the basic safety objective of "Life Safety" performance under the DBE and "Collapse Prevention" performance under the MCE; or enhanced objectives can be considered, such as "Immediate Occupancy" performance under the DBE and "Life Safety" performance under the MCE. Here, three design criteria are established for the basic safety objective (BSO): (1) limit the peak story drift ratio to 2.5% rad and the residual story drift ratio to 1.0% rad under the DBE; (2) limit the peak story drift ratio and the residual story drift ratio to 5.0% rad under the MCE; (3) keep the bracing and connections associated with the dampers linear elastic under the DBE ground motions. Higher performance objectives, with smaller story drift limits, can be

established if desired.

Step 2.Design MRF for a specified level of base shear design strength. The MRF is designed to satisfy the strength criteria for a conventional MRF from seismic design provisions, such as ASCE 7–16, and the characteristics of the MRF (e.g., initial stiffness, mode shapes, and natural frequencies) are obtained.

Step 3.Determine damper placement configuration in structure and estimate appropriate value for $\alpha_{\rm b}=k_{\rm b}/k_{\rm 0}$. Based on the damper placement configuration in the structure, $k_{\rm b}$ is the overall stiffness of the associated bracing in the damping system in the global horizontal direction. Therefore, $k_{\rm b}$ represents the total flexibility of the components in the complete damper force path, such as the braces, brace-gusset connections, damper-brace connections, damper-beam connections, and the

shortening and elongation of the columns of the damping system. k_0 is the MRF story stiffness in the global horizontal direction. α_b is used as an index for the flexibility of the complete damper force path. In general, $\alpha_b \geq 5$ is recommended to provide a relatively stiff design of the bracing to ensure the effectiveness of the damping devices.

Step 4.Size dampers to meet story drift criteria established in Step 1. As the MRF is designed only for the base shear design strength determined in Step 2, damping devices are added and sized to control the story drifts. An elastic-static analysis procedure (ESAP) can be used for the analysis needed to determine the damper properties. The ESAP idealizes the nonlinear viscous damper-brace component as an equivalent linear elastic-viscous model, and using this model, the effective stiffness and equivalent damping of the structure can be estimated. The details of the ESAP will be discussed later in Section 2.3. The story drift criteria established in Step 1 should be satisfied by the MRF with the selected damper sizes. As shown in Fig. 3, the dampers can be increased in size if needed. If unpractical dampers sizes are required to meet the drift criteria, then the MRF should be re-designed with an increased level of base shear design strength, otherwise the story drift criteria in Step 1 should be re-established.

Step 5. Design of damping system. With the damper sizes established in Step 4 and the story drift criteria established in Step 1, the bracing of the damping system can be designed for the maximum expected damper force for the specified story drift. The design of the damping system includes the design details for the braces, beams, columns, brace-beam-column connections, brace-damper connections, and damper-beam connections. The overall flexibility (i.e., α_b) of the complete damper force path should be assessed. The procedure should go back to Step 4 to resize the dampers for a smaller α_b if the actual value of α_b for the asdesigned damping system is smaller than the value established in Step 3.

Step 6. Check strength of MRF. The MRF was designed for the specified level of base shear design strength in Step 2, which did not account for the effects of the damper forces on the MRF. The in-phase behavior of the damper forces with the story drifts could increase internal forces in the columns of the MRF, which requires the strength of the columns of the MRF to be checked for the effects of damper forces. The MRF should be strengthened if needed.

2.3. Elastic-static analysis procedure for MRF structure with nonlinear viscous dampers

The elastic-static analysis procedure (ESAP) used in Step 4 of the SDP is as follows:

Step A1. Equivalent linearization of nonlinear viscous damper-brace component as an equivalent linear elastic-viscous model. The force-velocity relationship for a nonlinear viscous damper is as:

$$f_{\rm d} = C_{\alpha} sgn(v_{\rm d}) |v_{\rm d}|^{\alpha} \tag{1}$$

where f_d is the damper force; v_d is the damper velocity; $\operatorname{sgn}(v_d)$ gives the direction of the damper velocity; C_α is the damping coefficient; and α is the velocity exponent with value 0.44 in the manuscript. This type of nonlinear viscous dampers is a representative damper product manufactured by Taylor Devices Inc. This equivalent linearization is described in detail by Dong [19]. For a specified target story drift, the equivalent effective stiffness $k_{\rm eq}$ and viscous damping coefficient $C_{\rm eq}$ for the equivalent linear elastic-viscous model in each story can be determined as Eqs. (2) and (3). Given damper properties (damping coefficient C_α and velocity exponent α) and bracing stiffness $k_{\rm b}$, the equivalent properties (i.e., $k_{\rm eq}$ and $C_{\rm eq}$) are expressed as functions of natural frequency $\omega_{\rm s}$ and estimated target story drift $u_{\rm ds}$ of the structure.

$$k_{\rm eq} = \frac{\left(C_a \omega_{\rm s}^a (u_{\rm ds})^{a-1}\right)^2}{\left(C_a \omega_{\rm s}^a (u_{\rm ds})^{a-1}\right)^2 + \left(k_{\rm b}\right)^2} k_{\rm b} \tag{2}$$

$$C_{\text{eq}} = \frac{C_a \omega_s^{\alpha - 1} (u_{\text{ds}})^{\alpha - 1}}{\left(C_a \omega_s^{\alpha} (u_{\text{ds}})^{\alpha - 1}\right)^2 + (k_b)^2} (k_b)^2$$
(3)

Step A2. Eigenvalue analysis of structure (i.e., MRF with added dampers) using the equivalent linear elastic-viscous model for nonlinear viscous damper-brace component. The total stiffness matrix of the structure, K_t , should be updated by including the equivalent effective stiffness of the equivalent linear elastic-viscous model for the damping system, $K_{\rm eq}$, as follows, $K_t = K_0 + K_{\rm eq}$, where K_0 is the initial stiffness matrix of the MRF. With the updated K_t , the updated mode shapes and natural frequencies of the structure can be obtained through eigenvalue analysis.

Step A3. Calculate equivalent damping ratio ξ_{eq} using lateral force energy method [19,20] as:

$$\xi_{\text{eq}} = \frac{1}{4\pi} \frac{\pi \omega_1 \sum_{i} \left[C_{\text{eq},i} \cdot \left(\phi_{i,1} - \phi_{i-1,} \right)^2 \right]}{0.5 \cdot \left(\mathbf{\Phi}_1^T \mathbf{K}_i \mathbf{\Phi}_1 \right)}$$
(4)

where ω_1 is the undamped natural circular frequency of the structure with added dampers for the first mode; Φ_1 is the mode shape for the first mode and $\phi_{i,\ 1}$ is the mode coordinates at the i^{th} floor of Φ_1 ; K_t is the effective stiffness matrix of the MRF with added dampers, from Step A2; $C_{\text{eq},\ i}$ is the damping coefficient for the *equivalent linear elastic-viscous model* of i^{th} story based on the specified target story drift limit. The effective damping ξ_{eff} of the structure equals the sum of the equivalent damping ξ_{eq} and inherent damping of the building ξ_{I} .

Step A4. Equivalent lateral force (ELF) procedure or response spectrum analysis (RSA) procedure for linear analysis of MRF with added dampers. In this study, the ELF procedure was used to estimate the seismic base shear and floor displacement response of the structure with added dampers. The equivalent damping (Eq. (4)) was based on the first mode frequency and mode shape of the structure. The seismic base shear (V) and equivalent lateral forces ($F_{\rm ELF}$) based on the first mode shape can be calculated as follows:

$$V = \frac{\Gamma_1}{R_1} C_s W \tag{5}$$

$$\mathbf{F}_{\text{ELF}} = \frac{\Gamma_1}{R_1} C_s W \cdot \mathbf{\Phi}_1 \tag{6}$$

where Γ_1 is the modal participation factor of the first mode; B_1 is the damping coefficient for effective damping $\xi_{\rm eff}$, W is the seismic weight of the structure; C_s is the seismic response coefficient determined as follows:

$$C_s = \begin{cases} \frac{S_{DS}}{R/I_e} & \text{for } T_1 < T_s \\ \frac{S_{D1}}{T_1(R/I_e)} & \text{for } T_1 \ge T_s \end{cases}$$
 (7)

where $T_s = 0.6$ seconds. Since the purpose of the analysis is to determine the floor lateral displacements and the corresponding story drifts, the response modification factor R is taken as R = 1.0, when the *equal displacement approximation* is used to establish the for floor displacements. Static analysis should be performed under the equivalent lateral forces from Eq. (6) to estimate the floor displacements.

Steps A1 through A4 of the ESAP should be repeated for each set of trial damper sizes until the story drift criteria are met. The ESAP uses only linear static analysis based on the widely-used ELF procedure and RSA procedure, which enables a preliminary evaluation of seismic performance of the MRF with added dampers, in terms of story drift, without complex nonlinear analyses.

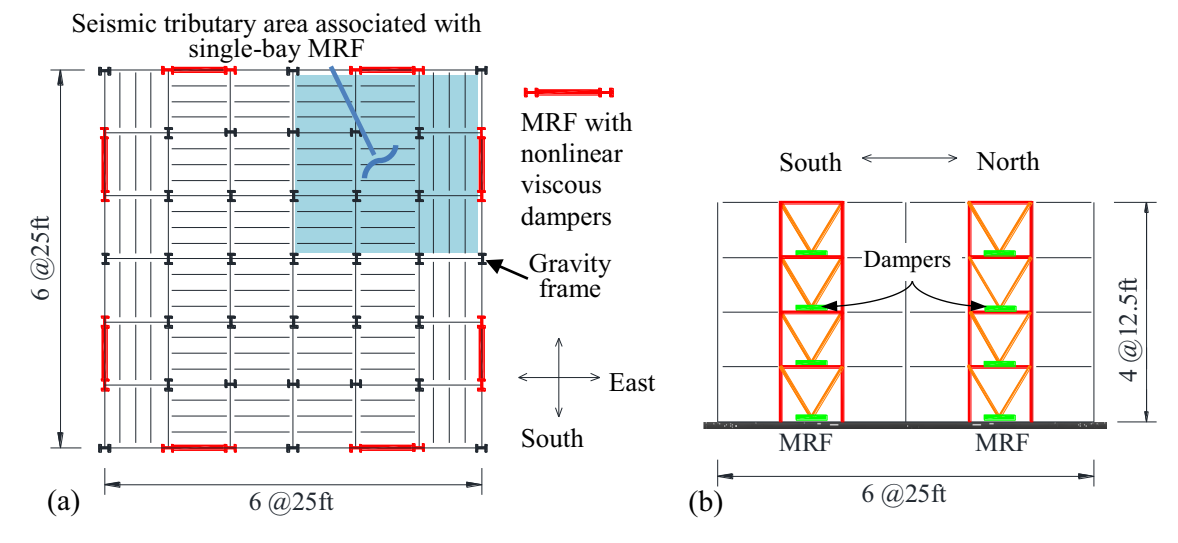


Fig. 4. 4-story MRF building with nonlinear viscous dampers: (a) plan view; (b) section view.

3. Validation of SDP for 4-story steel MRFs with nonlinear viscous dampers

3.1. Design of 4-story steel MRFs

The SDP is validated for a 4-story example steel MRF building with nonlinear viscous dampers. The example building is assumed to be located on a stiff soil site in Los Angeles. Fig. 4 shows the floor plan and section view of the 4-story example MRF building with nonlinear viscous dampers. The building has 8 perimeter MRFs to resist lateral forces, and the dampers are placed directly in each story of the MRFs of the example building. The design of the 4-story example building focuses on the design of a single-bay MRF with nonlinear viscous dampers placed directly in each story of the MRF.

To compare the seismic response and performance of the MRF building without dampers with the MRF building with dampers, three types of MRFs are designed for the building: (1) two special moment resisting frames (SMRF) without dampers, denoted SMRF-A and SMRF-B; where SMRF-A is designed to satisfy the strength criteria of ASCE 7–16 and a story drift limit of 1.5% radians, and SMRF-B is designed to satisfy the strength criteria of ASCE 7-16 and a story drift limit of 2.0% radians; (2) MRFs that satisfy the strength criteria of ASCE 7-16 and use nonlinear viscous dampers to control the story drift, denoted MRF-D100V, which is designed to resist 100% of the required base shear design strength of ASCE 7-16 without satisfying the story drift limit; (3) MRFs designed for reduced base shear design strength and use nonlinear viscous dampers to control the story drift, denoted MRF-D75V, MRF-D60V, MRF-D50V, and MRF-D40V, which are designed to resist 75%, 60%, 50%, and 40% of the required base shear design strength of ASCE 7–16, respectively.

The required base shear design strength of the SMRF-A and SMRF-B, MRF-D100V, MRF-D75V, MRF-D60V, MRF-D50V, and MRF-D40V was

determined using the ELF procedure based on an estimated design period $T_{\text{des}} = 0.9 \text{ s}$ for the 4-story MRF building, the strength reduction factor R=8, and the ASCE 7-16 design response spectrum (with parameters $S_{DS}=1.0~g$ and $S_{D1}=0.6~g$). The members of the MRFs were sized for the strength criteria through elastic analysis with the ASCE 7–16 load combinations described using the SAP 2000 program, ASTM A992 steel beams were selected for the MRFs so that the lightest section with a section modulus equal to or slightly greater than the required section modulus, according to AISC [21,22], were selected. ASTM A992 steel W14 sections were used for the columns. Considering a standard available length of 30 ft for the steel members, the same section was used for the columns in the first and second stories, and the same section was used for the columns in the third and fourth stories. For SMRF-A and SMRF-B, the member sections were increased to satisfy the 1.5% and 2.0% rad story drift limits with the displacement amplification factor C_d = 5.5, respectively. Table 1 gives the sections and the associated weight of the MRFs. MRF-D75V, MRF-D60V, MRF-D50V, MRF-D40V are 14%, 27%, 37%, and 42% lighter than MRF-D100V, respectively, while MRF-D100V is 49% and 37% lighter than SMRF-A and SMRF-B, respectively.

Table 2 gives the properties of the MRFs, including the base shear design strengths at the design period, $V_{\rm des}$ (from Eq. (4), with $\Gamma_1=1.0$, $B_1=1.0$, and $T_{\rm des}=0.9$ seconds); the modal periods, $T_{\rm n}$ (n=1,2,3,4); the story drifts based on the displacement amplification factor $C_{\rm d}=5.5$, $\theta_{\rm des}$; the story drifts at initial yielding of the MRF, $\theta_{\rm y}$; and the actual response modification factors, $R_{\rm act}$, which accounts for inherent material overstrength and the effects of resistance factors in the LRFD method, as the MRFs are assumed to be designed for strength using ASCE 7–16 and the LRFD method of AISC 360–10 [21]. $R_{\rm act}$ is calculated as $R_{\rm act}=S_{\rm a,\ T}/S_{\rm a,\ Y}$, where $S_{\rm a,\ T}$ is the design spectral acceleration at the first period of the structure, T_1 , and $S_{\rm d,\ Y}$ is the spectral acceleration corresponding to the base shear that causes initial yielding of the MRF under a pattern of lateral force based on the first mode shape. $\theta_{\rm v}$ is the story drift from

Table 1Design of SMRFs and MRFs for 4-story example building.

Structure	Column				Beam				Weight
	1st story	2nd story	3rd story	4th story	1st floor	2nd floor	3rd floor	4th floor	(kips)
SMRF-A	W14 × 370		W14 × 311		W36 × 210	W36 × 210	W36 × 150	W24 × 76	50.2
SMRF-B	$W14 \times 257$		W14 \times 211		$W36\times150$	$W33\times141$	$W33\times118$	$W24\times 62$	35.2
MRF-D100V	W14 × 193		$W14 \times 145$		W30 × 116	$W30\times108$	$W27 \times 84$	$W21 \times 44$	25.7
MRF-D75V	W14 × 159		W14 \times 132		$W27 \times 94$	$W27 \times 94$	$W21\times 73$	W21 \times 44	22.2
MRF-D60V	$W14 \times 132$		$W14 \times 109$		$W27 \times 84$	$W27\times 84$	$W21 \times 62$	W18 \times 40	18.8
MRF-D50V	W14 \times 120		$W14 \times 82$		$W24\times 76$	$W24\times 76$	$W21\times 57$	$W18\times40$	16.3
MRF-D40V	W14 × 109		$W14 \times 82$		$W24 \times 68$	$W24 \times 62$	$W21 \times 44$	W18 \times 40	14.9

Table 2Properties of SMRFs and MRFs for 4-story example building.

а	Base shear at T_{des} (kN)	Modal period (s)			Design story drift ratio, $\theta_{\rm des}$ (% rad) ($R=8,C_{\rm d}=5.5$)			Story drift ratio at initial yielding, $\theta_{\rm y}$ (% rad)			R _{act}			
		T_1	T_2	T_3	T_4	1st story	2nd story	3rd story	4th story	1st story	2nd story	3rd story	4th story	
SMRF-A	193	1.12	0.40	0.20	0.13	1.24	1.52	1.51	1.38	0.53	0.66	0.66	0.60	2.7
SMRF-B	193	1.42	0.49	0.25	0.16	1.56	1.97	2.00	1.75	0.55	0.69	0.70	0.61	3.3
MRF-D100V	193	1.70	0.59	0.30	0.19	2.09	2.75	3.01	2.79	0.54	0.71	0.78	0.72	4.5
MRF-D75V	145	2.00	0.67	0.32	0.20	2.49	3.31	3.62	3.33	0.56	0.74	0.81	0.75	5.2
MRF-D60V	116	2.22	0.74	0.35	0.22	2.77	3.64	4.07	3.90	0.54	0.72	0.81	0.78	5.9
MRF-D50V	96	2.48	0.79	0.37	0.23	3.09	4.17	4.69	4.30	0.57	0.77	0.87	0.79	6.2
MRF-D40V	77	2.68	0.83	0.38	0.23	3.40	4.72	5.31	4.77	0.52	0.72	0.81	0.73	7.6

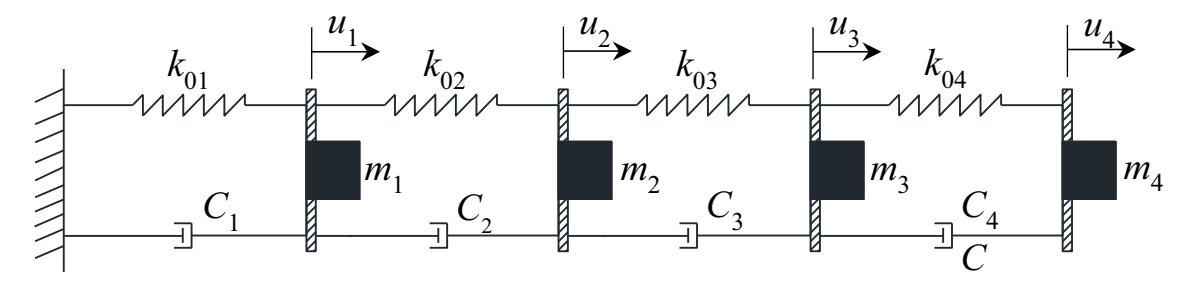


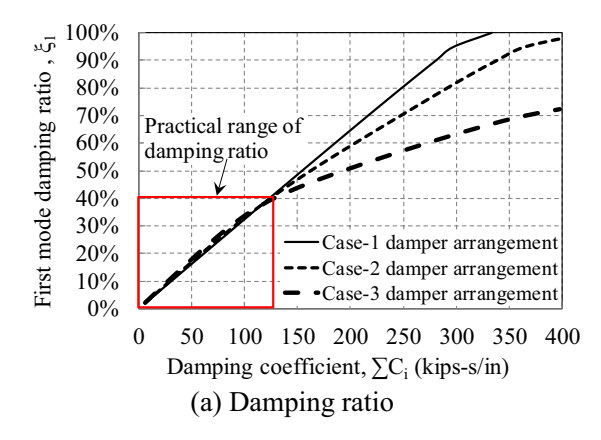
Fig. 5. State-space model for 4-story MRF structure with dampers and associated rigid bracing.

analysis with a pattern of lateral force (E) based on the first mode shape with increasing magnitude, along with constant gravity loads (D and L), using the load combination 1.4D+0.5L+1.0E, until initial yielding occurs in the beams of the MRF. It is seen that the MRFs have similar values of θ_y . SMRF-A and SMRF-B have smaller $R_{\rm act}$ than each of the other MRF. $R_{\rm act}$ increases as the base shear design strength decreases from MRF-D100V to MRF-D40V.

3.2. Effects of damper arrangement on damping ratio

To control the story drifts of the MRF-D100V, MRF-D75V, MRF-D60V, MRF-D50V, MRF-D40V structures, nonlinear viscous dampers were added and sized for the MRFs using the SDP. Practical arrangement of dampers in a building structure is usually based on the assumption that the effectiveness of each damper is proportional to the peak damper deformation or peak damper velocity. Researchers also have studied methods of arranging dampers, e.g., Ribakov and Gluck [23] showed that the optimal arrangement of damping coefficients for a seven-story shear building is proportional to the story stiffness, Takewaki [24] showed that the optimal damper arrangement is an almost uniform distribution of dampers with uniform properties for a six-story shear

building with uniform distribution of story drifts, and Ashour [25] suggested placing dampers at the locations that will maximize the damping ratio for the fundamental mode of a multi-story building structure. Based on these findings, three cases of damper arrangement in the MRF are studied: Case-1, story stiffness proportional dampers; Case-2, uniform dampers; and Case-3, nonproportional dampers. In Case-1, the dampers are arranged so that the damping coefficients are proportional to the story stiffnesses of the MRF structure without dampers; in Case-2, the dampers are arranged so that the damping coefficients are the same in each story of the structure; and in Case-3, the dampers are arranged so that the damping coefficients in the second, third, and fourth stories are two, three, and two times the damping coefficient in the first story, respectively. The effects of damper arrangement on the dynamic properties of the 4-story example MRF building are investigated through eigenvalue and eigenvector analysis of a state-space representation of the MRF with the dampers. In the state-space representation of the MRF with the dampers, the braces that connect the dampers to seismic mass DOF are assumed to be rigid. The story stiffness of the MRF is represented by an elastic spring, and the damper in each story of the structure are represented by a dashpot with a damping coefficient C_i (i = 1, 2, 3, 4), as shown in Fig. 5. Therefore, the structure is



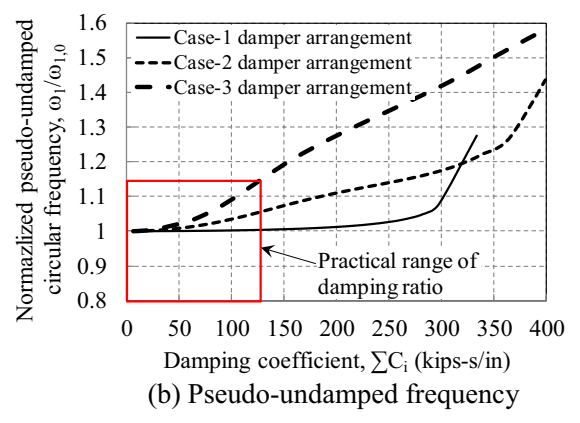


Fig. 6. Effects of damper arrangement on damping ratio and pseudo-undamped natural frequency.

Table 3Category-A MRFs: Designed for 1.5% rad story drift with Case-1 damper arrangement.

C_{α} (kips-s/in) $\alpha = 0.44$),			1st mode damping $\xi_{\rm eq}$ (%)	Damping coefficient B_1	$R_{\rm act}/B_1$
1st story	2nd story	3rd story	4th story		•	
92	64	46	38	28	1.74	2.58
99	68	51	44	39	2.07	2.51
99	69	51	43	46	2.27	2.60
95	65	49	44	55	2.56	2.42
99	66	50	47	63	2.80	2.71
	a = 0.44 1st story 92 99 99	1st story 2nd story 92 64 99 68 99 69 95 65	$\begin{array}{c ccccccccccccccccccccccccccccccccccc$	$\begin{array}{c ccccccccccccccccccccccccccccccccccc$	$\begin{array}{c ccccccccccccccccccccccccccccccccccc$	$\begin{array}{c ccccccccccccccccccccccccccccccccccc$

Table 4 Category-B MRFs: Designed for 1.5% rad story drift with Case-2 damper arrangement.

Category-B MRFs	C_{lpha} (kips-s/in) $lpha=0.44$,			1st mode damping ξ_{eq} (%)	Damping coefficient B_1	$R_{\rm act}/B_1$
	1st story	2nd story	3rd story	4th story			
MRF-D100V-b	59	59	59	59	28	1.75	2.57
MRF-D75V-b	63	63	63	63	38	2.05	2.54
MRF-D60V-b	63	63	63	63	45	2.25	2.62
MRF-D50V-b	62	62	62	62	55	2.55	2.43
MRF-D40V-b	64	64	64	64	63	2.80	2.71

idealized as having four lateral DOF at each floor level. The model does not include the inherent damping of the building.

Fig. 6 shows the effects of damper arrangement on damping ratio and pseudo-undamped natural circular frequency of the MRF-D100V structure with dampers and associated rigid bracing. Fig. 6(a) shows the first mode damping ratio (ξ_1) versus the total added damping coefficient $(\sum_{i=1}^{4} C_i)$ of the structure. It is seen that the first mode damping ratio of the structure with Case-1 damper arrangement increases nearly linearly with an increase in the damping coefficients, while the first mode damping ratios of the structure with Case-2 and Case-3 damper arrangements increase nonlinearly with an increase in the damping coefficients. Overall, Fig. 6(a) shows that the first mode damping ratio for the structure with dampers depends on the size and arrangement of the dampers in the structure, although that the effect of the damper arrangement on the damping ratio is small when the damping ratio is smaller than 40%. This result suggests that within a practical damping ratio range for the MRF-D100V structure, the arrangement of dampers is not that impactful. Fig. 6(b) shows the first mode pseudo-undamped natural circular frequency (ω_1) normalized by natural circular frequency $(\omega_{1,0})$ of the MRF-D100V structure without dampers versus the total added damping coefficient $(\sum_{i=1}^4 C_i)$ of the structure. It is seen that ω_1/ω_1 o is greater than 1.0 and increases with an increase in the damping coefficients. The increase is most obvious for Case-3 damper arrangement. These results show that the pseudo-undamped natural circular frequency of a structure with added nonproportional damping will be greater than the natural circular frequency of the structure without added damping. For Case-1 and Case-2 damper arrangements, the increase of the natural frequency of the structure in within 5% for a practical damping ratio within 40%, which could provide an estimate that MRF column internal forces will increase about 10% to account for

the in-phase behavior of the damper forces with the story drifts.

4. Dynamic analysis results and performance evaluation

Nonlinear viscous dampers were added and sized for the various MRF designs using the SDP to limit the story drift to be less than either 1.5% or 2.0% radians under the DBE. Case-1 and Case-2 damper arrangement were used in the study. An overall bracing stiffness with $k_{\rm b}/k_{01}=10$ was used for the designs, where k_{01} is the MRF first story stiffness in the global horizontal direction. A total of four categories of MRF structures with supplemental nonlinear dampers are considered in this study, and their design properties are shown in Table 3 through Table 6. Category-A MRFs are designed for 1.5% rad story drift limit with Case-1 damper arrangement (See Table 3); Category-B MRFs are designed for 1.5% rad story drift limit with Case-2 damper arrangement (See Table 4); Category-C MRFs are designed for 2.0% rad story drift limit with Case-1 damper arrangement (See Table 5); Category-D MRFs are designed for 2.0% rad story drift limit with Case-2 damper arrangement (See Table 6). The story drifts, added damping from the dampers, ξ_{eq} , damping coefficient, B_1 , and the value of $R = R_{act}/B_1$ from the SDP are given in the tables.

Nonlinear models for the 4-story MRF structures were built using the OpenSees program [26]. Nonlinear dynamic time history analyses (NDTHA) were performed using a set of eight ground motions to assess the seismic response and performance of the MRF structures with nonlinear viscous dampers in terms of story drifts, beam and column plastic rotations, floor accelerations, and column internal forces. Table 7 gives the set of eight ground motions, which were scaled to the design basis earthquake (DBE) and maximum considered earthquake (MCE) hazard levels. Details of the selection and scaling of the set ground motions can be found in [19,27]. Fig. 7 compares the median spectrum

Table 5Category-C MRFs: Designed for 2.0% rad story drift with Case-1 damper arrangement.

Category-C MRFs	C_{α} (kips-s/in) $\alpha = 0.44$,			1st mode damping $\xi_{\rm eq}$ (%)	Damping coefficient B_1	$R_{\rm act}/B_1$
	1st story	2nd story	3rd story	4th story			
MRF-D100V-c	52	36	26	21	15	1.34	3.36
MRF-D75V-c	65	44	33	29	23	1.57	3.31
MRF-D60V-c	69	48	35	30	28	1.73	3.40
MRF-D50V-c	66	45	34	30	35	1.95	3.18
MRF-D40V-c	76	50	38	36	42	2.16	3.52

Table 6Category-D MRFs: Designed for 2.0% rad story drift with Case-2 damper arrangement.

Category-D MRFs	C_{α} (kips-s/in) $\alpha = 0.44$,			1st mode damping $\xi_{\rm eq}$ (%)	Damping coefficient B_1	$R_{\rm act}/B_1$
	1st story	2nd story	3rd story	4th story			
MRF-D100V-d	33	33	33	33	15	1.34	3.36
MRF-D75V-d	41	41	41	41	22	1.56	3.31
MRF-D60V-d	44	44	44	44	28	1.73	3.40
MRF-D50V-d	42	42	42	42	34	1.93	3.18
MRF-D40V-d	48	48	48	48	41	2.14	3.52

Table 7Earthquake ground motions used for NDTHA of 4-story MRF structures.

ID	Earthquake Event			Record	Scale factor	
	Year	Mw	Name		DBE	MCE
1	1979	6.5	Imperial Valley	H-E03140	1.44	2.31
2	1992	7.3	Landers	YER360	2.06	3.31
3	1989	6.9	Loma Prieta	HSP090	1.72	2.76
4	1989	6.9	Loma Prieta	WVC000	1.25	2.02
5	1989	6.9	Loma Prieta	WVC270	1.11	1.78
6	1994	6.7	Northridge	RRS318	0.66	1.06
7	1994	6.7	Northridge	SCE018	0.59	0.95
8	1979	5.9	Westmorland	PTS315	1.88	3.02

of the set with DBE and MCE uniform hazard spectrum (UHS) that represent the seismic hazard at the building site in this study. The UHS were developed using the ground motion intensity model from Campbell and Bozorgnia [28] and the OpenSHA program [29], where the DBE and MCE UHS has 10% and 2% probability of exceedance (POE) in 50 years,

respectively. Notably, the median spectrum of the set closely matches the UHS.

4.1. Story drift response

Fig. 8 through Fig. 11 compare mean peak story drifts from the NDTHA with story drifts from the SDP (using ELF) for the MRFs with nonlinear viscous dampers designed for 1.5% rad story drift limit under the DBE and MCE. Fig. 12 through Fig. 15 compare mean peak story drifts from NDTHA with story drifts from the SDP (using ELF) for the MRFs with nonlinear viscous dampers designed for 2.0% rad story drift limit under the DBE and MCE. It is shown that the story drifts from the SDP are close to the mean peak story drifts from the NDTHA under the DBE and MCE. For the Category-A and Category-C MRFs with Case-1 damper arrangement, the maximum mean peak story drifts from the NDTHA of various MRFs are less than the results from the SDP and therefore satisfy the 1.5% rad and 2.0% rad story drift under the DBE ground motions, respectively. For the MRFs with Case-2 damper arrangement, except the MRF-D50V-b and MRF-D40V-b structures, the

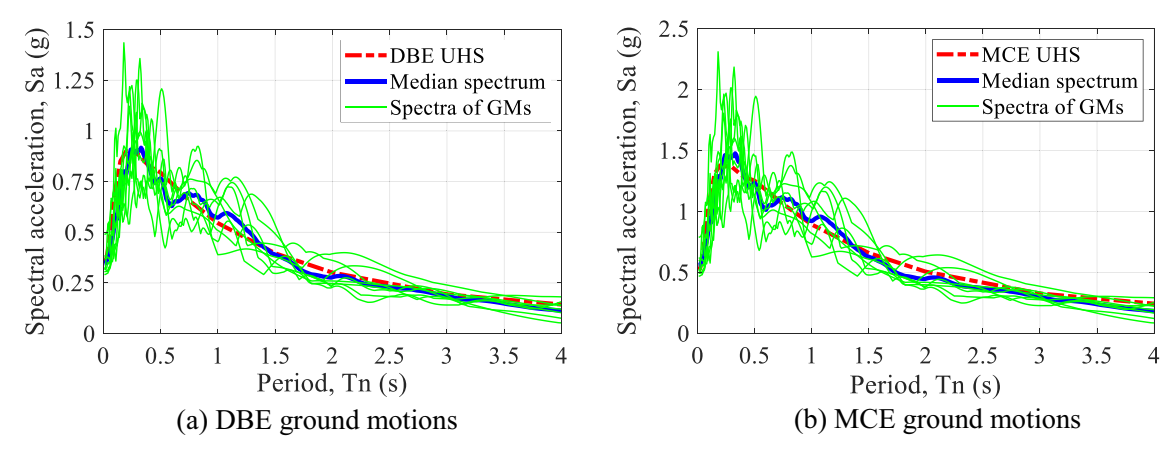


Fig. 7. DBE and MCE level ground motions for NDTHA.

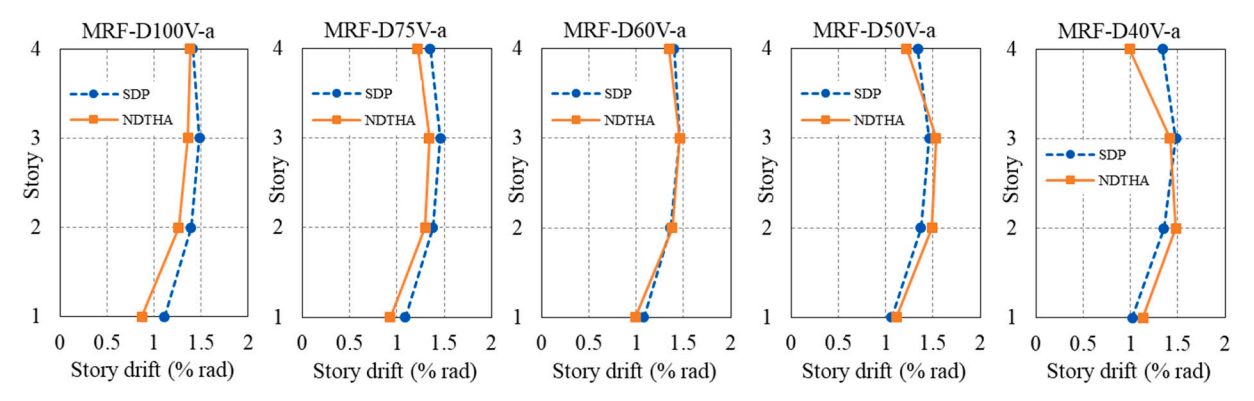


Fig. 8. Story drift comparison between SDP and NDTHA: MRFs Category-A under DBE.

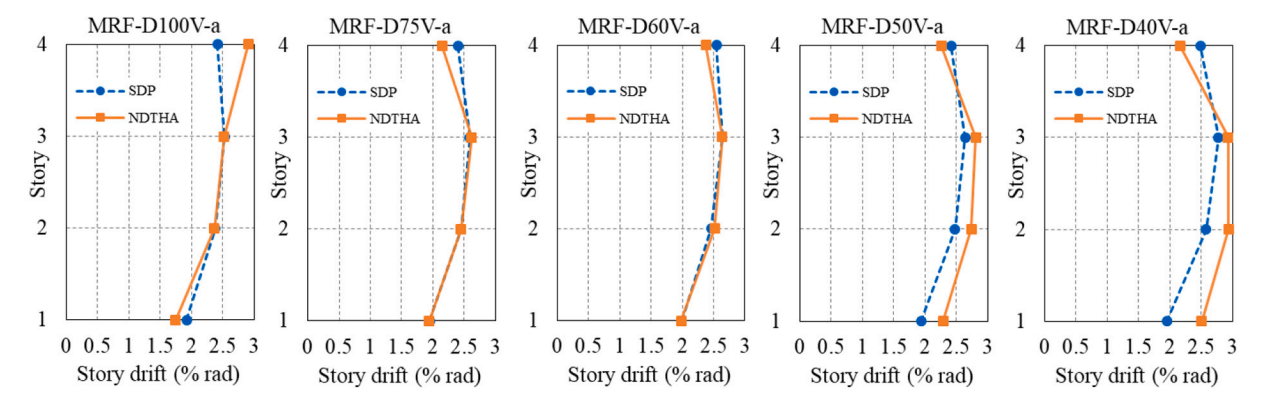


Fig. 9. Story drift comparison between SDP and NDTHA: MRFs Category-A under MCE.

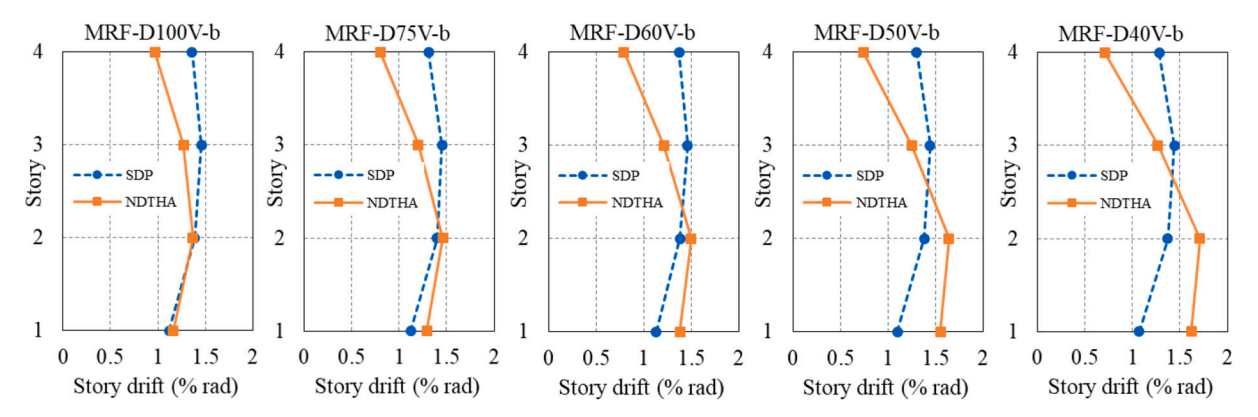


Fig. 10. Story drift comparison between SDP and NDTHA: MRFs Category-B under DBE.

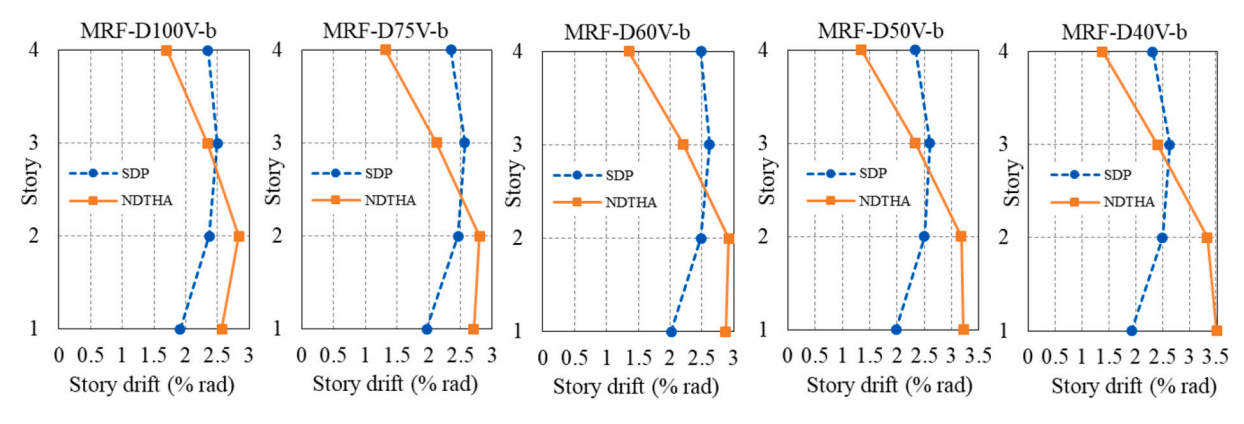


Fig. 11. Story drift comparison between SDP and NDTHA: MRFs Category-B under MCE.

maximum mean peak story drifts from the NDTHA of the various Category-B and Category-D MRFs are less than the results from the SDP and therefore also satisfy the 1.5% and 2.0% rad story drift under the DBE ground motions, respectively.

However, differences in the story drift response of the MRFs with the two cases of damper arrangement can be seen. As shown in Figs. 8–9 and Figs. 12–13, for the MRFs with Case-1 damper arrangement (i.e., Category-A and Category-C MRFs), the distribution over the stories of the mean peak story drifts from the NDTHA are similar to the results from the SDP, i.e., the maximum mean peak story drifts are located in the upper stories of the structure, under both the DBE and MCE. Particularly, the SDP accurately predicts the story drift results for each story of the Category-A MRFs under the both the DBE and MCE. For the MRFs with Case-2 damper arrangement (i.e., Category-B and Category-D MRFs), the lower stories have the maximum mean peak story drifts, and

are slightly larger than the results from the SDP, as demonstrated in Figs. 10–11 and Figs. 14–15. These results demonstrate that damper arrangement configuration affects the accuracy of the SDP more than the specified target story drift. Overall, the SDP gives story drift results much closer to the results from the NDTHA for the MRFs with Case-1 damper arrangement than for the MRFs with Case-2 damper arrangement under the DBE and MCE ground motions. The SDP gives similar accuracy for the MRFs sized with 1.5% rad story drift and the MRFs sized with 2.0% rad story drift, therefore, can be used for multi-performance seismic design of MRF structures with nonlinear viscous dampers.

4.2. Local plastic rotation response

The column plastic rotations and beam plastic rotations under the DBE and MCE ground motions are examined here. Fig. 16 compares the

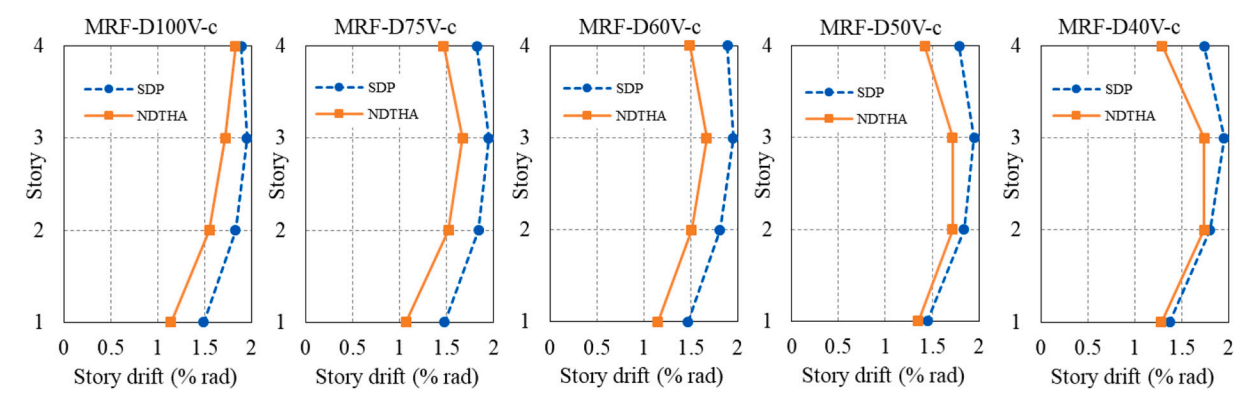


Fig. 12. Story drift comparison between SDP and NDTHA: MRFs Category-C under DBE.

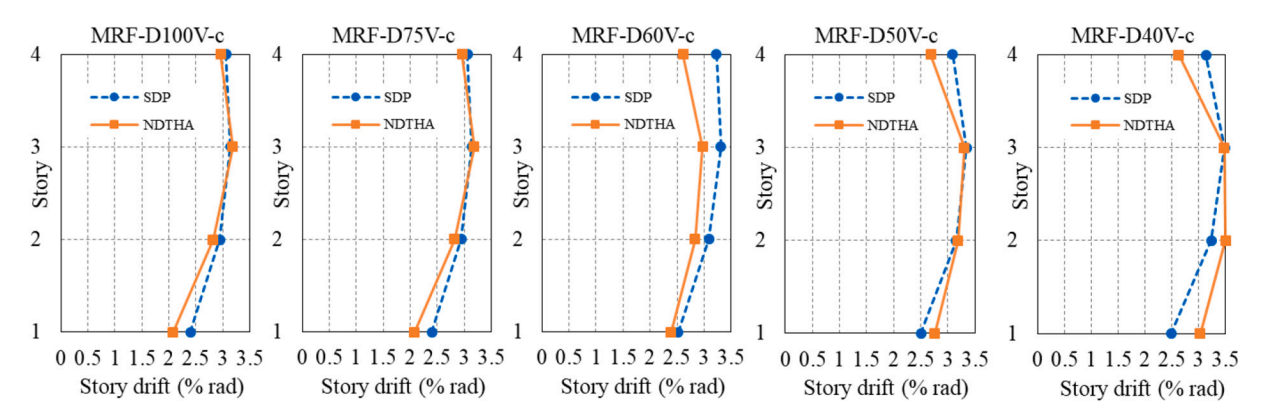


Fig. 13. Story drift comparison between SDP and NDTHA: MRFs Category-C under MCE.

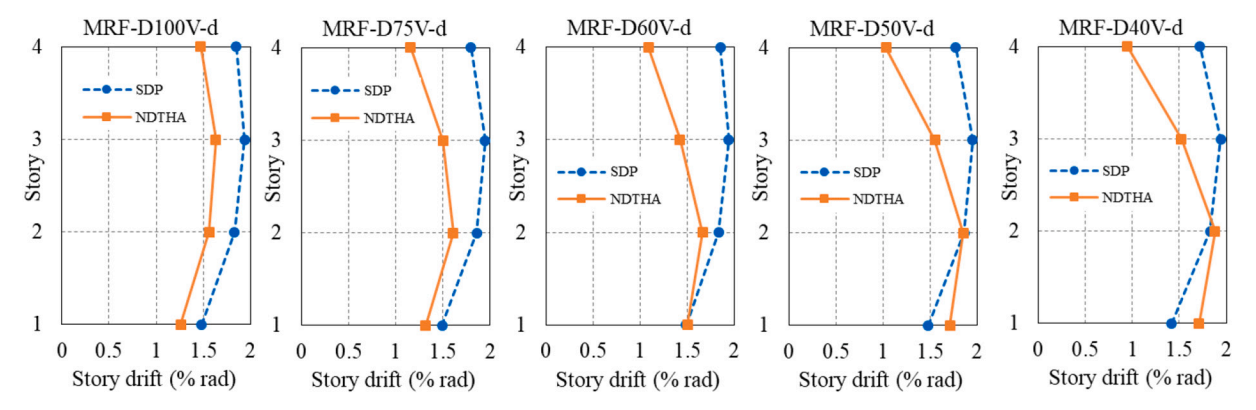


Fig. 14. Story drift comparison between SDP and NDTHA: MRFs Category-D under DBE.

mean peak first story column plastic rotations of the Category-A and Category-B MRFs (i.e., MRFs with dampers sized for 1.5% rad story drift with Case-1 and Case-2 damper agreements) with the mean peak first story column plastic rotation of SMRF-A, from the NDTHA. Under the DBE ground motions, SMRF-A and the Category-A and Category-B MRFs have very small column plastic rotations (less than 0.1% radians), which indicates the first story columns of SMRF-A and the MRFs with dampers remained essentially elastic. Under the MCE ground motions, the mean peak column plastic rotations of the first story columns are 0.12%, 0.17%, 0.30%, 0.30%, and 0.34% rad for the MRF-D100V-a, MRF-D75V-a, MRF-D60V-a, MRF-D50V-a, and MRF-D40V-a structures, respectively, and are 0.28%, 0.32%, 0.43%, 0.51%, and 0.58% rad for the MRF-D100V-b, MRF-D75V-b, MRF-D60V-b, MRF-D50V-b, and MRF-D40V-b structures, respectively, which are larger than the mean peak column plastic rotation of 0.12% rad for SMRF-A, which demonstrates that the

value of the mean peak column plastic rotation for the MRFs with dampers increases as the base shear design strength decreases. Nevertheless, the mean peak column plastic rotations of all the structures nearly remained within the residual story drift ratio limit that can affect the moving components of buildings such as doors, windows, and sliding partitions [30–32], which validates that Category-A and Category-B MRFs have comparable performance as the SMRF-A in terms of column plastic rotations.

Figs. 17 and 18 compare the mean peak beam plastic rotations of Category-A and Category-B MRFs with the same results of SMRF-A from the NDTHA under the DBE and MCE ground motions, respectively. Figs. 17(a) and 18(a) show that Category-A MRFs (i.e., MRFs with Case-1 damper arrangement) have smaller mean peak beam plastic rotations than SMRF-A under the DBE and MCE ground motions. Figs. 17(b) and 18(b) show that the mean peak beam plastic rotations of Category-B

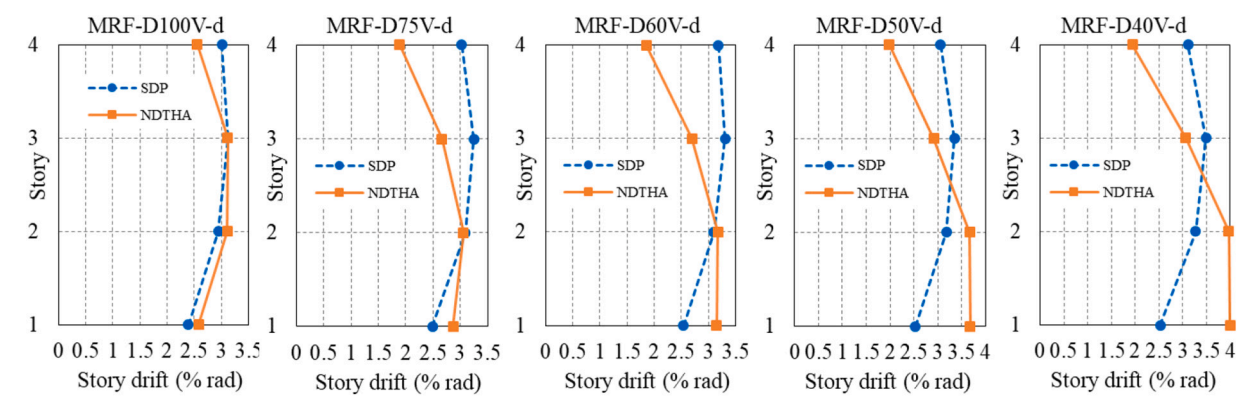


Fig. 15. Story drift comparison between SDP and NDTHA: MRFs Category-D under MCE.

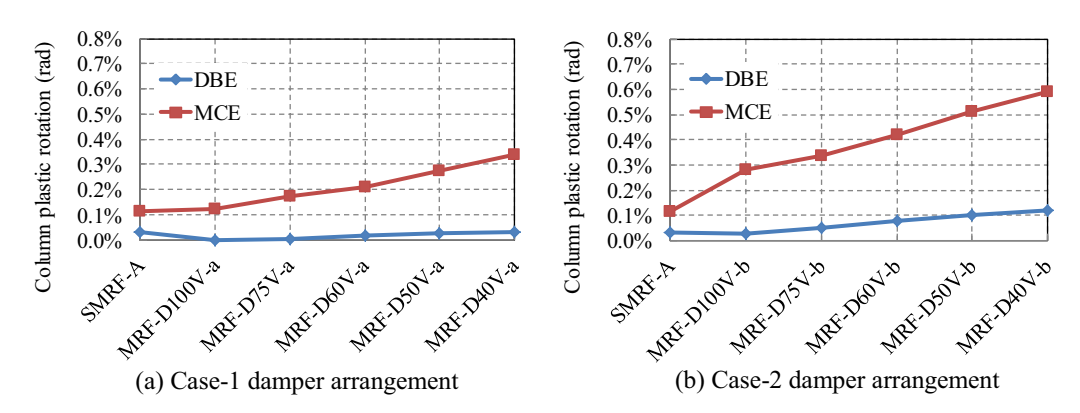


Fig. 16. Mean peak column plastic rotations: SMRF-A, Category-A and Category-B MRFs.

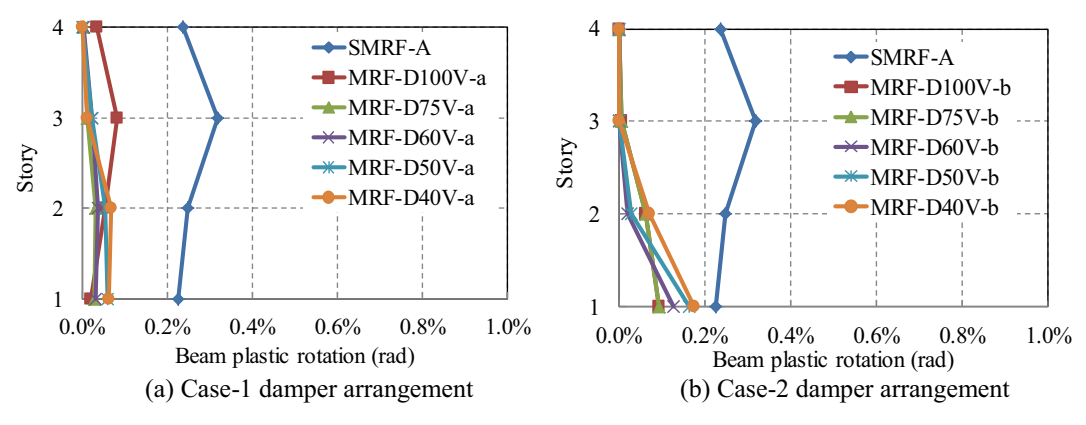


Fig. 17. Mean peak beam plastic rotation under DBE: SMRF-A, Category-A and Category-B MRFs.

MRFs (MRFs with Case-2 damper arrangement) are larger for the first floor than for other floors, but are slightly smaller than those of SMRF-A under the DBE and greater than those of SMRF-A under the MCE.

Fig. 19 compares the mean peak column plastic rotations of the first story columns of Category-C and Category-D MRFs (i.e., MRFs with dampers sized for 2.0% rad story drift with Case-1 and Case-2 damper agreements) with the same results of SMRF-B. Similar to Category-A and Category-B MRFs, the mean peak column plastic rotation of Category-C and Category-D increases as the base shear design strength decreases. The mean peak column plastic rotations are approximately 0.1% rad or less under the DBE ground motions, which indicates the first story columns of the MRFs with dampers remained essentially elastic. The mean peak column plastic rotations of Category-D MRFs are larger than those of Category-C MRFs and SMRF-B under the DBE and MCE ground

motions.

Figs. 20 and 21 compare the mean peak beam plastic rotations of Category-C and Category-D MRFs with the same results of SMRF-B from the NDTHA under the DBE and MCE ground motions, respectively. Similar to Category-A MRFs, Category-C MRFs have smaller mean peak beam plastic rotations than SMRF-B under both the DBE and MCE ground motions. The mean peak beam plastic rotations of Category-D MRFs are larger for the first floor than for other floors, but are slightly smaller than those of SMRF-B under the DBE and slightly greater than those of SMRF-B under the MCE ground motions.

The seismic performance of the MRFs with dampers and SMRFs are evaluated as: (1) the MRFs with Case-1 damper arrangement have better performance than MRFs with Case-2 damper arrangement under both the DBE and MCE; (2) the MRFs with Case-1 and Case-2 damper

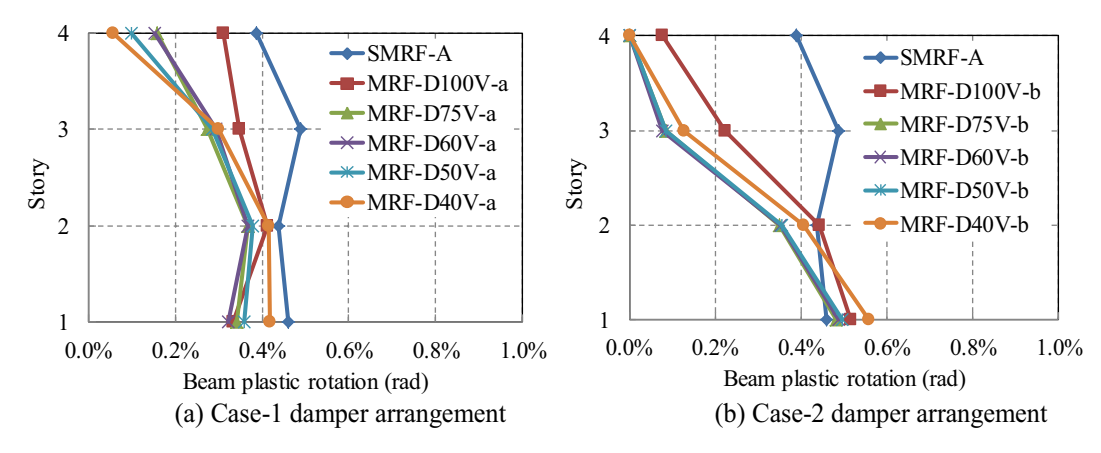


Fig. 18. Mean peak beam plastic rotations under MCE: SMRF-A, Category-A and Category-B MRFs.

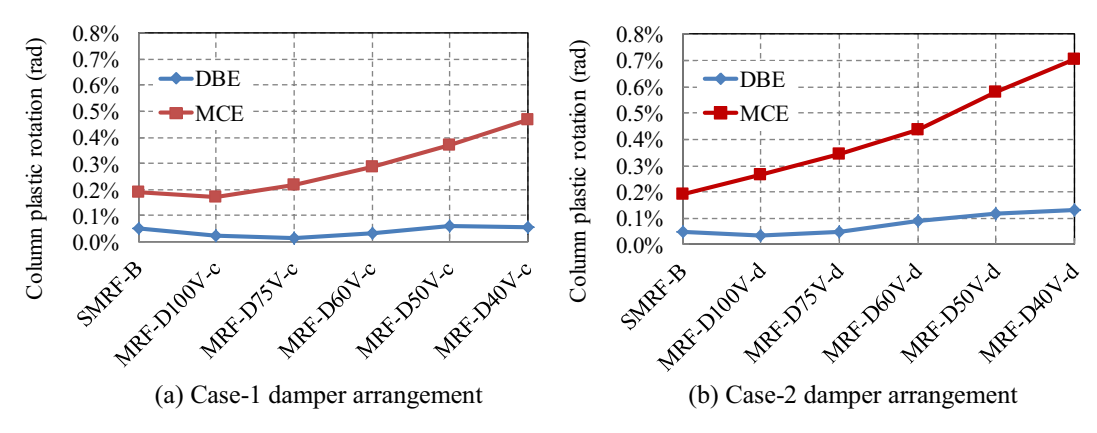


Fig. 19. Mean peak column plastic rotations: SMRF-B, Category-C and Category-D MRFs.

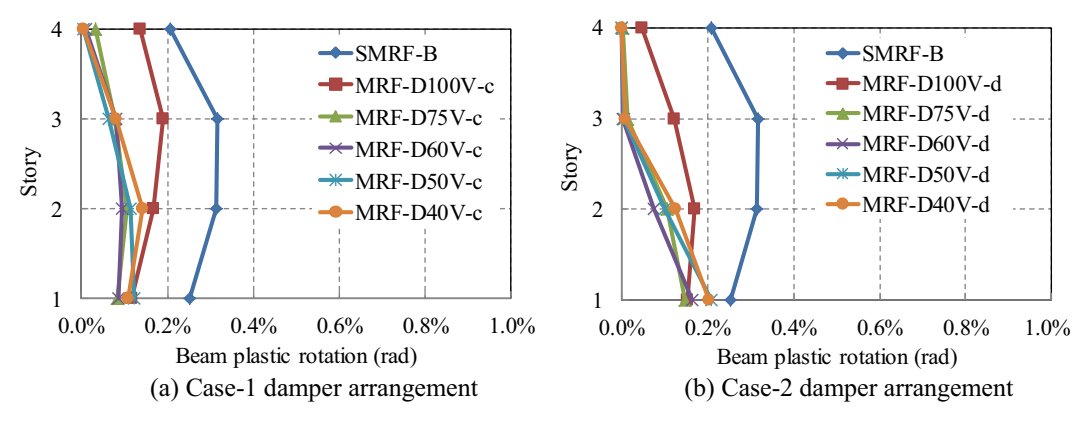


Fig. 20. Mean peak beam plastic rotations under DBE: SMRF-B, Category-C and Category-D MRFs.

arrangement have better seismic performance than SMRF-A and SMRF-B under the DBE; (3) the MRFs with Case-1 and Case-2 damper arrangements have seismic performance similar to that of SMRF-A and SMRF-B under the MCE; (4) the MRFs with dampers designed with various base shear design strengths have similar seismic performance under the DBE, and under the MCE, the MRFs designed with a higher level of base shear design strength have better seismic performance.

4.3. Floor acceleration response

Figs. 22-25 summarize the mean peak floor accelerations from the NDTHA for the SMRFs and the MRFs with dampers. It is seen that the mean peak floor accelerations of the MRFs with dampers are much

smaller than the SMRFs under the DBE and MCE. The mean peak floor accelerations of the MRFs with dampers decrease as the base shear design strength level decreases. The mean peak floor accelerations of the fourth floor of the MRF-D100V-a, MRF-D75V-a, MRF-D60V-a, MRF-D50V-a, and MRF-D40V-a structures are 56%, 46%, 43%, 38%, and 30% of that of SMRF-A under the DBE, and are 70%, 62%, 59%, 51%, and 45% of that of SMRF-A under the MCE. The mean peak floor accelerations of the fourth floor of the MRF-D100V-c, MRF-D75V-c, MRF-D60V-c, MRF-D50V-c, and MRF-D40V-c structures are 74%, 63%, 56%, 51%, and 44% of that of the SMRF-B under the DBE, and are 70%, 64%, 58%, 54%, and 47% of that of SMRF-B under the MCE. The mean peak floor accelerations of the MRFs with Case-2 damper arrangement are slightly smaller than those of the MRFs with Case-1 damper arrangement.

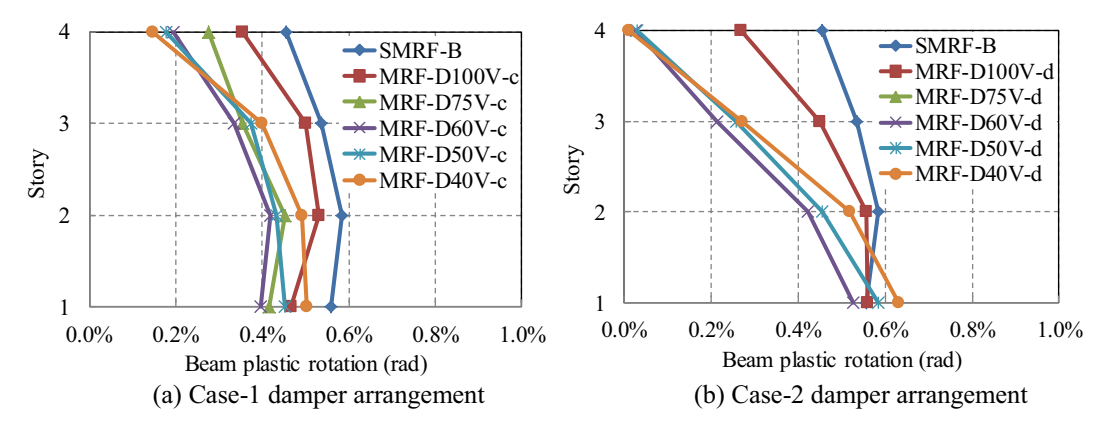


Fig. 21. Beam mean plastic rotations under MCE: SMRF-B, Category-C and Category-D MRFs.

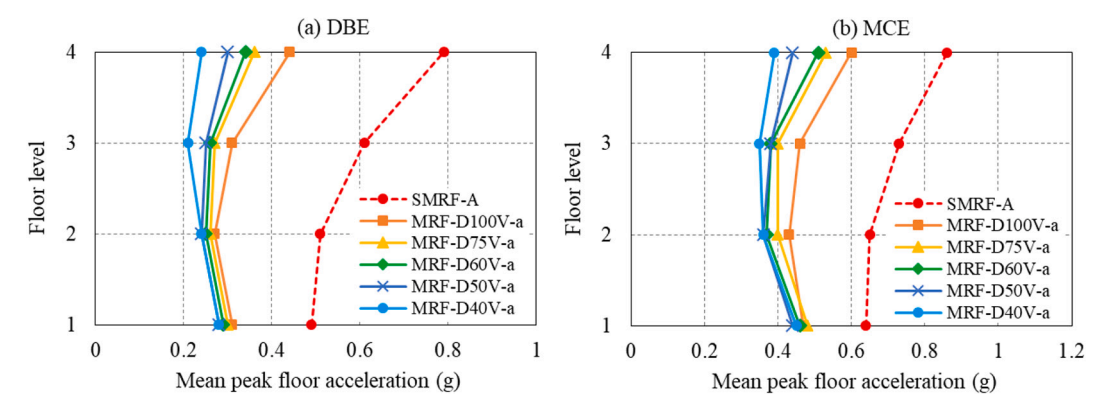


Fig. 22. Mean peak floor accelerations from NDTHA: SMRF-A and Category-A MRFs.

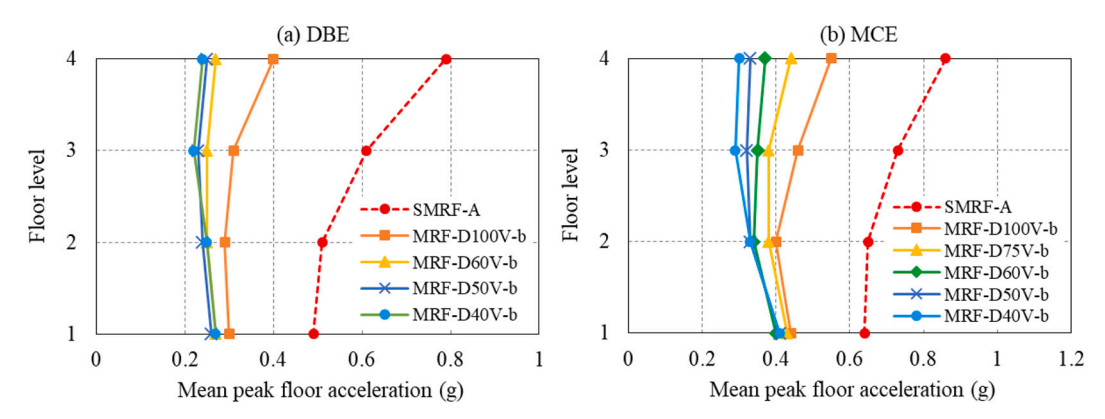


Fig. 23. Mean peak floor accelerations from NDTHA: SMRF-A and Category-B MRFs.

Therefore, in terms of mean peak floor accelerations, the MRFs with Case-2 damper arrangement achieved better seismic performance than the SMRFs and MRFs with Case-1 damper arrangement.

4.4. MRF column internal forces

The internal forces in the columns of the MRFs with dampers are compared with those in the columns of the SMRFs and evaluated in this section. Fig. 26 shows the combination of axial forces and bending moments that develops in the first story columns of SMRF-A and SMRF-B under DBE ground motion record H-E03140. The P-M strength curve of the columns based on AISC 360–10 for beam-column members subjected to flexure and axial forces is also plotted in the Figures. The nominal axial and flexural strength of the column section was used in the AISC

360–10 column strength formulae. Fig. 26 shows that the combination of axial forces and bending moments in the columns of SMRF-A and SMRF-B slightly exceed the P-M strength curve, which indicates the columns of SMRF-A and SMRF-B yield and develop plastic rotations under the DBE ground motion record H-E03140.

Fig. 27 shows the combination of axial force and bending moment in the columns of Category-A MRFs (i.e., MRFs sized for 1.5% rad story drift with Case-1 damper arrangement) under the DBE ground motion record H-E03140. Fig. 27(a) and (b) show that the combination of axial forces and bending moments in the columns of the MRF-D100V-a and MRF-D75V-a structures are mostly within the P-M strength curve, which indicates the columns satisfy the strength requirement under the DBE including the effects of the damper forces. Fig. 27(c) and (d) show the combination of axial forces and bending moments in the columns of the

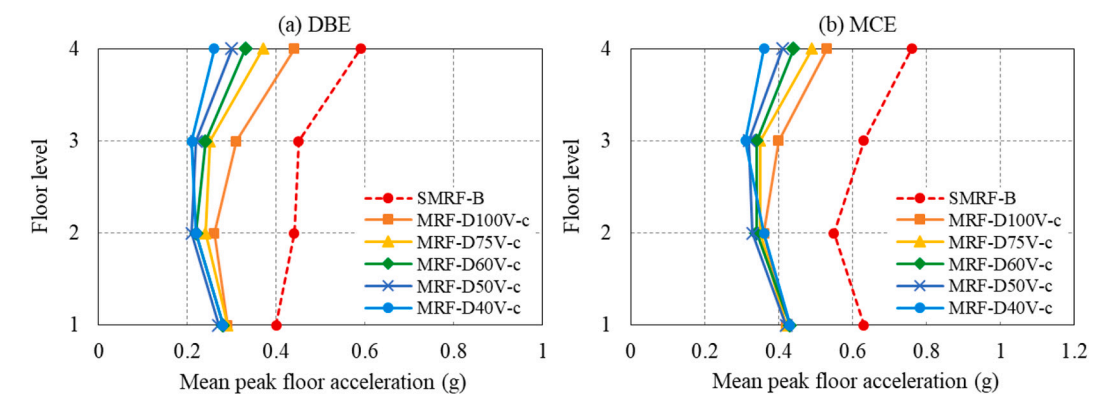


Fig. 24. Mean peak floor accelerations from NDTHA: SMRF-B and Category-C MRFs.

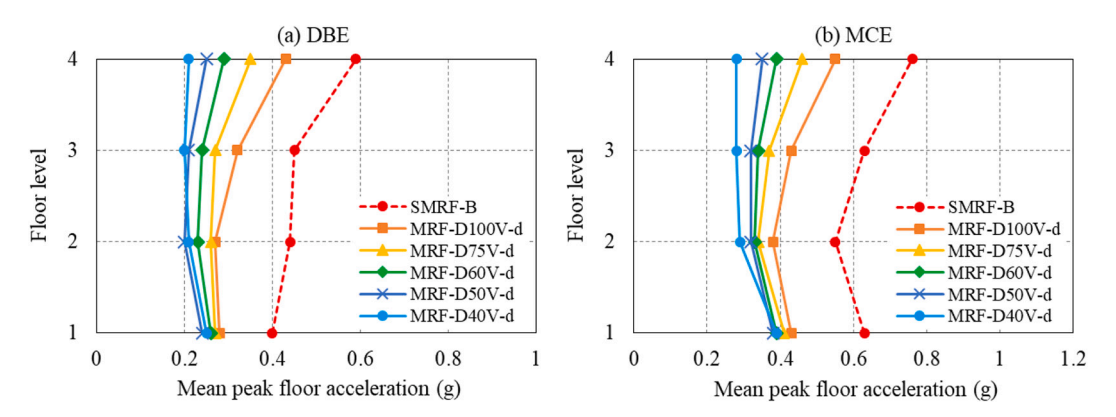


Fig. 25. Mean peak floor accelerations from NDTHA: SMRF-B and Category-D MRFs.

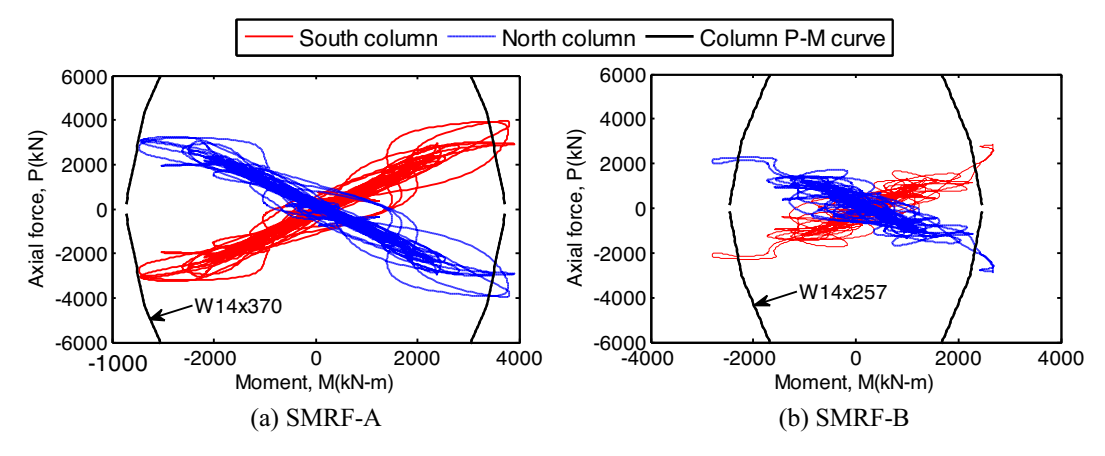


Fig. 26. Internal forces in columns of SMRF-A and SMRF-B under DBE record H-E030140.

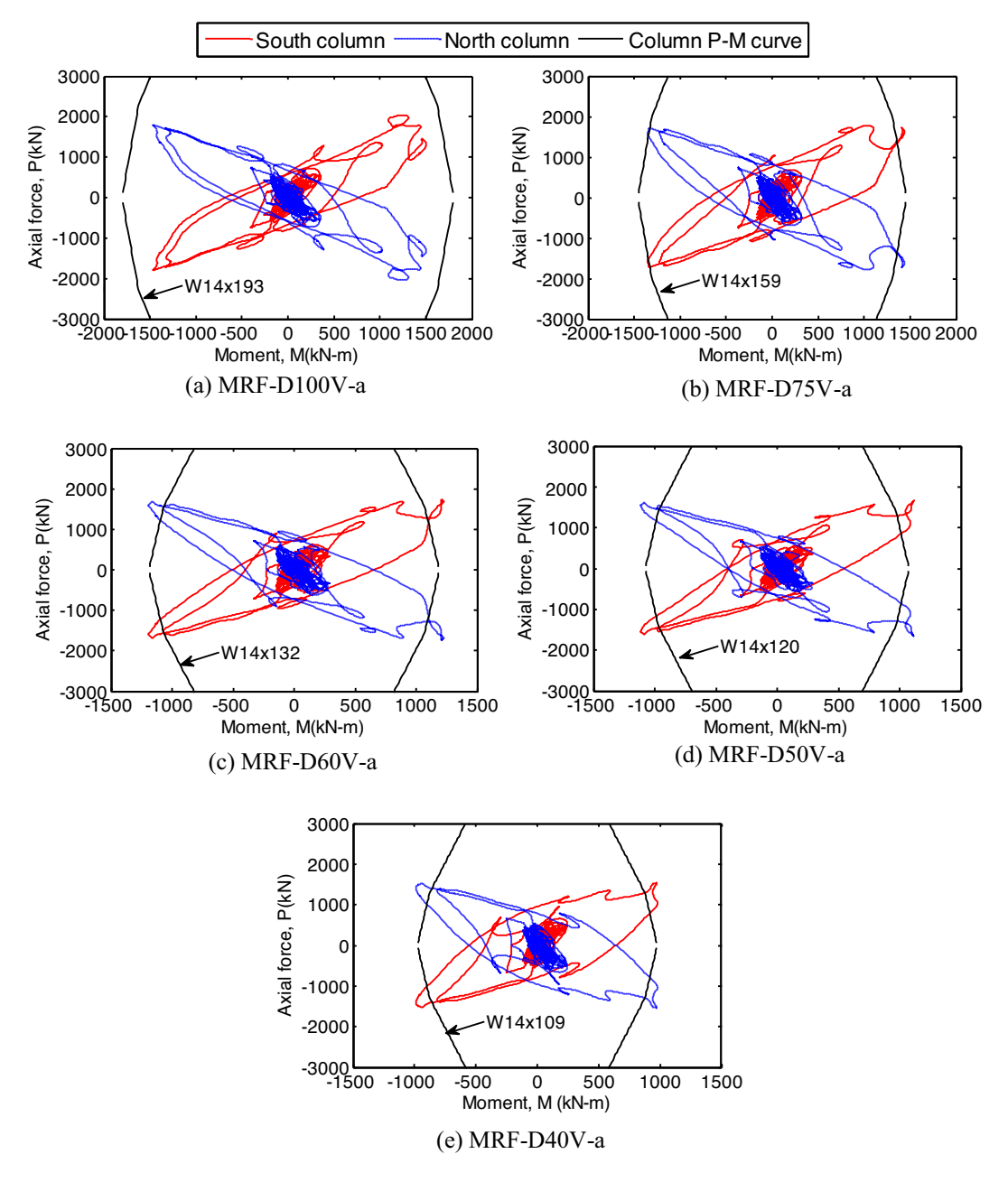
MRF-D60V-a, MRF-D50V-a, and MRF-D40V-a structures exceed the P-M strength curve, which indicates the columns, similar to the columns of SMRF-A and SMRF-B, yield and develop plastic rotations under the DBE including the effects of the damper forces, since lighter sections were used for the columns of the MRFs designed with reduced base shear design strength.

Fig. 28 shows the combinations of axial force and bending moment in the columns of the MRFs sized for 2.0% rad story drift with Case-1 damper arrangement under the DBE ground motion record H-E03140. Due to a larger story drift demand on the MRFs sized for 2.0% rad story drift than the MRFs sized for 1.5% rad story drift, the combinations of axial force and bending moment in the columns of all the MRFs exceed the P-M strength curve, and therefore, yield and develop larger plastic

rotations under the DBE.

5. Summary and conclusions

This paper presented a simplified design procedure (SDP) for seismic design of low-rise steel MRF structures with nonlinear viscous dampers. For selected performance objectives and associated story drift based design criteria, the SDP enables an integrated design of the MRF and damping system to be performed. In the SDP, the MRF is designed for strength criteria and the damping system is sized for drift criteria. Unlike the current analysis procedures for structures with dampers in ASCE 7–16, where the effective period and effective damping ratio are computed as a function of the ductility demand on the structure, the SDP



 $\textbf{Fig. 27.} \ \ \textbf{Internal forces in columns of Category-A MRFs under DBE record H-E030140}.$

uses only elastic analysis of a linear model of the MRF. The linear model of the MRF uses an equivalent linearized model of the damping system. The SDP is consistent with the analysis procedures in ASCE 7–16 for seismic design of conventional structures without dampers. The SDP was validated using results for a 4-story example steel MRF building with nonlinear viscous dampers. The MRFs were designed for various base shear design strength levels (i.e., 100%, 75%, 60%, 50% and 40% of the required base shear design strength of ASCE 7–16), and nonlinear viscous dampers were sized and added to the MRFs to control the story drift response. Two cases of damper arrangements were studied. Nonlinear dynamic time history analyses (NDTHA) were performed. The main findings and conclusions are as follows:

(1) The MRF structures with dampers have better performance than SMRFs without dampers under the DBE and have performance similar to that of the similarly designed SMRFs without dampers under the MCE.

- (2) The MRF structures with dampers can be designed with reduced base shear design strength (60%, 50%, and 40%) to achieve equivalent seismic performance of SMRF structures without dampers and MRF structures with dampers designed with required (i.e.,100% and 75%) base shear design strength.
- (3) The SDP enables an integrated design between the seismic forceresisting system (SFRS) and damping system in a way that SFRS is designed for the compliance of strength criteria and the damping system is added for the compliance of drift criteria.
- (4) The SDP reduces the complexity of the analysis procedures for structural system with dampers in ASCE 7–16 for seismic design of structures with nonlinear viscous dampers with validated accuracy.

Authorship statement

All persons who meet authorship criteria are listed as authors, and all

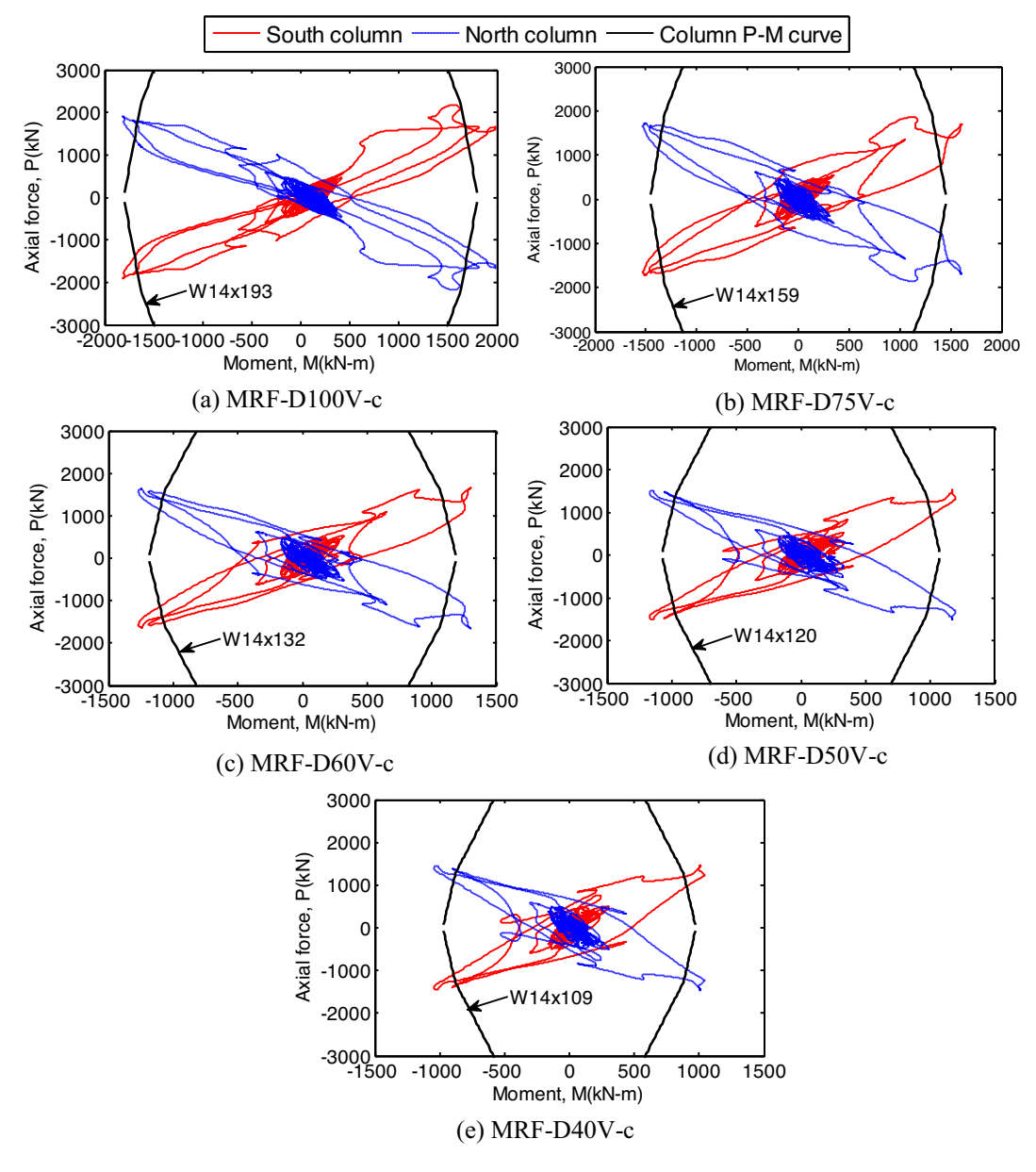


Fig. 28. Internal forces in columns of Category-C MRFs under DBE record H-E03140.

authors certify that they have participated sufficiently in the work to take public responsibility for the content, including participation in the concept, design, analysis, writing, or revision of the manuscript. Furthermore, each author certifies that this material or similar material has not been and will not be submitted to or published in any other publication before its appearance in the *Journal of Constructional Steel Research*.

Declaration of Competing Interest

The authors declare that they have no known competing financial interests or personal relationships that could have appeared to influence the work reported in this paper.

Acknowledgments

This paper is based upon work supported by from National Natural Science Foundation of China with grant No. 52078385 and Shanghai Pujiang Program (Project No. 20PJ1414000). Support was also provided

by National Science Foundation, Award No. CMS-0936610 in the George E. Brown, Jr. Network for Earthquake Engineering Simulation Research (NEESR) program.

References

- [1] M.D. Symans, F.A. Charney, A.S. Whittaker, M.C. Constantinou, C.A. Kircher, M. W. Johnson, R.J. McNamara, Energy dissipation systems for seismic applications: current practice and recent developments, J. Struct. Eng. 134 (1) (2008).
- [2] M.C. Constantinou, M.D. Symans, Experimental study of seismic response of buildings with supplemental fluid dampers, Struct. Design Tall Build. 2 (2) (1993) 93–132.
- [3] M.C. Constantinou, M.D. Symans, Seismic response of structures with supplemental damping, Struct. Design Tall Build. 2 (2) (1993) 77–92.
- [4] A.S. Whittaker, I.D. Aiken, D. Bergman, P.W. Clark, J.M. Cohen, J.M. Kelly, R. E. Scholl, Code Requirements for the Design and Implementation of Passive Energy Dissipation Systems. Proceedings of ATC 17–1 Seminar on Seismic Isolation, Passive Energy Dissipation, and Active Control. ATC, Redwood City, CA, 1993.
- [5] A.S. Whittaker, M.C. Constantinou, M.R. Oscar, M.W. Johnson, C.Z. Chrysostomou, Equivalent lateral force and modal analysis procedures of the 2000 NEHRP provisions for buildings with damping systems, Earthquake Spectra 19 (4) (2003).
- [6] ATC, NEHRP Guidelines for the Seismic Rehabilitation of Buildings. Applied Technology Council, FEMA-273, Federal Emergency Management Agency, Washington, DC, 1997.

- [7] Building Seismic Safety Council, NEHRP Recommended Provisions for Seismic Regulations for New Buildings and Other Structures, 1997 Edition, FEMA-302, Federal Emergency Management Agency, Washington, DC, 1998.
- [8] Building Seismic Safety Council, NEHRP Recommended Provisions for Seismic Regulations for New Buildings and Other Structures, 2003 Edition, FEMA-450, Federal Emergency Management Agency, Washington, DC, 2003.
- [9] O.M. Ramirez, M.C. Constantinou, A.S. Whittaker, C.A. Kircherm, C. Z. Chrysostomou, Elastic and inelastic seismic response of buildings with damping systems, Earthquake Spectra 18 (3) (2002).
- [10] O.M. Ramirez, M.C. Constantinou, J.D. Gomez, A.S. Whittaker, C.Z. Chrysostomou, Evaluation of simplified methods of analysis of yielding structures with damping devices, Earthquake Spectra 18 (3) (2002).
- [11] O.M. Ramirez, M.C. Constantinou, A.S. Whittaker, C.A. Kircher, M.W. Johnson, C. Z. Chrysostomou, Validation of the 2000 NEHRP provisions' equivalent lateral force and modal analysis procedures for buildings with damping systems, Earthquake Spectra (2003) 19(4).
- [12] Y. Lin, M.H. Tsai, J.S. Hwang, K.C. Chang, Direct displacement-based design for building with passive energy dissipation systems, Eng. Struct. 25 (2003).
- [13] J. Kim, H. Choi, Displacement-based design of supplemental dampers for seismic retrofit of a framed structure, J. Struct. Eng. 132 (6) (2006).
- [14] ASCE, Minimum Design Loads for Buildings and Other Structures (ASCE/SEI 7–16), American Society of Civil Engineers, Reston, VA, 2016.
- [15] Federal Emergency Management Agency (FEMA), Improvement of Nonlinear Static Seismic Analysis Procedures: FEMA-440, Federal Emergency Management Agency, Washington, DC, 2005.
- [16] O.M. Ramirez, M.C. Constantinou, C.A. Kircher, A.S. Whittaker, M.W. Johnson, J. D. Gomez, Development and Evaluation of Simplified Procedures for Analysis and Design of Buildings with Passive Energy Dissipation Systems, MCEER Report 00–0010, in: Multidisciplinary Center for Earthquake Engineering Research, University at Buffalo, State University of New York, Buffalo, NY, 2000.
- [17] N.M. Newmark, W.J. Hall, Earthquake Spectra and Design, Earth System Dynamics, 1982.
- [18] ASCE, Seismic Rehabilitation of Existing Buildings (ASCE/SEI 41–06), American Society of Civil Engineers, Reston, VA, 2007.
- [19] B. Dong, Large-Scale Experimental, Numerical, and Design Studies of Steel MRF Structures with Nonlinear Viscous Dampers under Seismic Loading, Lehigh University, Bethlehem, PA, PhD Dissertation, 2016.

- [20] R. Sause, G. Hemingway, K. Kasai, Simplified seismic response analysis of viscoelastic-damped frame structures, in: Proceedings of Fifth U.S. National Conference on Earthquake Engineering 1, EERI, 1994, pp. 839–848.
- [21] AISC, Specification for Structural Steel Buildings (ANSI/AISC 360–10), American Institute of Steel Construction, Chicago, Illinois, 2010.
- [22] AISC, Seismic Provisions for Structural Steel Buildings (ANSI/AISC 341–10), American Institute of Steel Construction, Chicago, Illinois, 2010.
- [23] Y. Ribakov, J. Gluck, Optimal design of ADAS damped MDOF structures, Earthquake Spectra 15 (2) (1999) 317–330.
- [24] I. Takewaki, Optimal damper placement for minimum transfer functions, Earthq. Eng. Struct. Dyn. 26 (11) (1997) 1113–1124.
- [25] S.A. Ashour, Elastic Seismic Response of Building with Supplemental Damping, Michigan University, Ann Arbor, USA, 1987.
- [26] OpenSees, Open System for Earthquake Engineering Simulation. Pacific Earthquake Engineering Research Center, University of California, Berkeley, 2012. Available at, http://opensees.berkeley.edu/.
- [27] B. Dong, R. Sause, J.M. Ricles, Seismic response and performance of a steel mrf building with nonlinear viscous dampers under DBE and MCE, J. Struct. Eng. (2016) 04016023, https://doi.org/10.1061/(ASCE)ST.1943-541X.0001482.
- [28] K.W. Campbell, Y. Bozorgnia, NGA ground motion model for the geometric mean horizontal component of PGA, PGV, PGD and 5% damped linear elastic response spectra for periods ranging from 0.01 to 10 s, Earthquake Spectra 24 (1) (2008) 139-171.
- [29] E.H. Field, T.H. Jordan, C.A. Cornell, OpenSHA: a developing community-modeling environment for seismic hazard analysis, Seismol. Res. Lett. 74 (4) (2003) 406–419
- [30] T.V. Galambos, B. Ellingwood, Serviceability limit states: deflection, J. Struct. Eng. 112 (1) (1986) 67–84.
- [31] B. Ellingwood, Earthquake risk assessment of building structures, Reliab. Eng. Syst. Saf. 74 (3) (2001) 251–262.
- [32] J. McCormick, H. Aburano, M. Ikenaga, M. Nakashima, Permissible residual deformation levels for building structures considering both safety and human elements, in: Proc., 14th World Conf. on Earthquake Engineering, Beijing, World Conference on Earthquake Engineering, 2008.